HHS Public Access

Author manuscript

Prostate. Author manuscript; available in PMC 2022 November 07.

Published in final edited form as:

Prostate. 2019 October ; 79(14): 1692–1704. doi:10.1002/pros.23894.

The role of WNT10B in normal prostate gland development and prostate cancer

Ikenna Madueke, MD, PhD[1], **Wen-Yang Hu, MD, PhD**[1], **Danping Hu, MD**[1], **Steven M. Swanson, PhD**[2], **Donald Vander Griend, PhD**[3,4], **Michael Abern, MD**[1,4], **Gail S. Prins, PhD**[1,3,4]

[1]Department of Urology, College of Medicine, University of Illinois at Chicago, Chicago, Illinois

[2]School of Pharmacy, University of Wisconsin-Madison, Madison, Wisconsin

[3]Department of Pathology, College of Medicine, University of Illinois at Chicago, Chicago, Illinois

[4]University of Illinois Cancer Center, Chicago, Illinois

Abstract

Background: WNT signaling is implicated in embryonic development, and in adult tissue homeostasis, while its deregulation is evident in disease. This study investigates the unique roles of canonical WNT10B in both normal prostate development and prostate cancer (PCa) progression.

Methods: Organ culture and rat ventral prostates (VPs) were used to study *Wnt10b* ontogeny and growth effect of WNT10B protein. PB-SV40 LTag rat VPs were utilized for *Wnt* expression polymerase chain reaction (PCR) array and immunohistochemistry. Human localized PCa tissue microarrays (TMAs) were investigated for differential *WNT10B* expression. Human RNA-seq data sets were queried for differential expression of *WNT10B* in metastatic and localized PCa. Knockdown of *WNT10B* in PC3 cells was utilized to study its effects on proliferation, stemness, epithelial to mesenchymal transition (EMT), and xenograft propagation.

Results: *Wnt10b* expression was highest at birth and rapidly declined in the postnatal rat VP. Exogenous WNT10B addition to culture developing VPs decreased growth suggesting an antiproliferative role. VPs from PB-SV40 LTag rats with localized PCa showed a 25-fold reduction in *Wnt10b* messenger RNA (mRNA) expession, confirmed at the protein level. Human PCa TMAs revealed elevated WNT10B protein in prostate intraepithelial neoplasia compared with normal prostates but reduced levels in localized PCa specimens. In contrast, RNA-seq data set of annotated human PCa metastasis found a significant increase in *WNT10B* mRNA expression compared with localized tumors suggesting stage-specific functions of WNT10B. Similarly, WNT10B mRNA levels were increased in metastatic cell lines PC3, PC3M, as well as in HuSLC, a PCa stem-like cell line, as compared with disease-free primary prostate epithelial cells.

Correspondence: Ikenna Madueke, MD, PhD, Department of Urology, College of Medicine, University of Illinois at Chicago, Chicago, IL 60612. imadue2@uic.edu.

CONFLICT OF INTERESTS

The authors declare that there are no conflict of interests.

SUPPORTING INFORMATION

Additional supporting information may be found online in the Supporting Information section.

WNT10B knockdown in PC3 cells reduced expression of EMT genes, MMP9 and stemness genes NANOG and SOX2 and markedly reduced the stem cell-like side population. Furthermore, loss of *WNT10B* abrogated the ability of PC3 cells to propagate tumors via serial transplantation.

Conclusions: Taken together, these results suggest a dual role for WNT10B in normal development and in PCa progression with opposing functions depending on disease stage. We propose that decreased WNT10B levels in localized cancer allow for a hyperproliferative state, whereas increased levels in advanced disease confer a stemness and malignant propensity which is mitigated by knocking down *WNT10B* levels. This raises the potential for WNT10B as a novel target for therapeutic intervention in metastatic PCa.

Keywords

development; metastasis; prostate cancer; prostate gland; WNT10B

1 | INTRODUCTION

The prostate is an exocrine male accessory sex gland consisting of branched ducts and secretory acini. Embryologically, it develops from the endodermal urogenital sinus (UGS), a process that is dependent on circulating fetal androgens.[1] While bud formation is the first morphological indication of prostate development, molecular signatures of prostate specification are evident before bud formation.[2] Until recently, the homeobox transcription factor *Nkx3.1* was the earliest known marker of prostate determination[3] and although a dependable marker of prostate identity, it is not essential for prostate formation.[4,5] This indicates that other signaling pathways may control prostate lineage commitment. *Wnt10b* was recently recognized as an early and more specific marker of prostate epithelial identity than *Nkx3.1* in that its expression is restricted to prostatic epithelium and, unlike *Nkx3.1*, is not found in bulbourethral glands.[6] This early and unique expression of WNT10B in prostate anlage suggests an important role for WNT10B in prostate development and raises the possibility that WNT10B may be deregulated in prostate diseases which frequently mimic development gone awry.

McNeal[7] proposed in 1978 that benign prostatic hyperplasia was a result of adult prostate stroma regaining a molecular signature similar to the embryonic prostatic mesenchyme and coined the phrase “embryonic reawakening potential” for adult prostatic disease. Prostate cancer (PCa), the most diagnosed noncutaneous male malignancy in the United States and second leading cause of cancer-related deaths in males, is also driven by the reawakening of developmental signals.[8,9] Although radical prostatectomy has a significant impact on patient survival in cases of localized cancer, a significant number of patients require additional treatment for local recurrence and previously undiagnosed metastatic lesions.[10] Since PCa is initially androgen-dependent, the current mainstay of treatment for locally advanced PCa or metastatic disease consists of surgical or chemical castration resulting in androgen ablation and consequent tumor regression. Unfortunately, the PCa cells invariably become androgen-independent, or castrate-resistant, leading to progression for which there is no curative treatment.[11,12] Increasing evidence suggests that evasion of conventional therapy with resultant progression is attributable, in part, to the presence of a very small population of androgen-independent PCa stem cells that repopulate regressed

tumors and drive progression.[7,13,14] It is thus noteworthy that β-catenin stabilization, as well as application of canonical WNT3A, has been shown to support ex vivo growth and maintenance of cultured PCa cells with stem-like characteristics.[15] In the present study, we investigated the role of WNT10B during prostate development and further probed its potential role in PCa progression.

WNT10B is a canonical WNT ligand implicated in the normal development, where it is expressed in the mouse embryonic yolk sac, fetal liver and hematopoietic cells,[16,17] and in oncogenesis of several organ systems. In cancers, WNT10B overexpression is documented in primary human breast carcinoma, breast carcinoma cell lines, and neuroblastoma cell lines.[18,19] In the rodent prostate, *Wnt10b* is the first *Wnt* gene expressed during development, occurring during prostate specification and initial urogenital sinus epithelium (UGE) budding.[20] Of note, *Wnt10b* expression is focally localized to epithelial cells at the distal tips of elongating ducts[20] where newly dividing and less differentiated cells reside during prostate morphogenesis.[21] This implicates a potentially important role for *Wnt10b* during prostate determination and control of stemness in the undifferentiated epithelium. This was separately supported by the ability of WNT10B, but not WNT3A, to drive prostatic fate during directed differentiation of human embryonic stem cells (hESCs) into prostate organoids in vitro.[22]

To further investigate the role of WNT10B in prostate development, the present studies characterized the spatiotemporal expression pattern of *Wnt10b* messenger RNA (mRNA) during rat prostate development and interrogated its role during prostate branching and ductal outgrowth using an organ culture system. Together, the findings implicate a growth-suppressive effect of WNT10B on the developing prostate. To investigate relevance to PCa, we examined the *Wnt* expression profile in a rat model of localized PCa which revealed significant downregulation of *Wnt10b* concomitant with an increased proliferative capacity of the adenocarcinoma. The human relevance of these findings was interrogated using a localized human PCa tissue microarray (TMA), RNA-seq data from prostatectomy, and metastatic specimens, and both in vitro and in vivo studies with the metastatic PCa cell line PC3. We provide evidence that WNT10B has a dual role in PCa progression dependent on the disease stage with downregulation during early disease which permits increased proliferation and re-expression in advanced PCa which promotes disease progression and metastasis by maintaining PCa stem-like cells.

2 | MATERIALS AND METHODS

2.1 | Animals

All animals were handled according to the principles and procedures of the Guiding Principles for the Care and Use of Animal Research and the experiments were approved by the Institutional Animal Care Committee. Timed pregnant female Sprague-Dawley rats from Harlan (Indianapolis, IN) were monitored for delivery and the day of birth was designated as day 0. The rats were killed by decapitation on postnatal day (pnd) 1, 3, 6, 10, 30, or 90, the UGS-prostate complexes were removed and the separate prostate lobes were micro dissected at 4°C and either frozen in liquid nitrogen or fixed for histology.

The probasin/TAg transgenic rat, developed on a Sprague-Dawley background, was obtained from Dr Tomoyuki Shirai, Nagoya City University, Japan.[23] Wild-type (WT) Sprague-Dawley rats were used as controls. Male rats were killed by decapitation at 25 weeks of age and the ventral prostate (VP) rapidly removed and either fixed for histologic analysis or snap-frozen for subsequent *Wnt* gene expression analysis.

For tumor development, PC3 cells were subcultured and injected (1×10^6 cells per 200 μL; 150 μL of phosphate-buffered saline and 50 μL high growth factor Matrigel per injection) subcutaneously (s.c.) into the flanks of nude mice following isoflurane anesthesia administration. Tumors were harvested after 30 days and individually weighed. For transplant studies, tumors were aseptically minced into ~1 mm^3 pieces in complete medium and transplanted into two sites, subcutaneously or underneath the renal capsule of nude mice. Transplanted grafts were harvested after 9 weeks, weighed and fixed in methacarn or flash-frozen for gene expression analysis. Host mice lungs, livers, and spleen were fixed to assess evidence of metastasis.

2.2 | Prostate organ culture

To examine the effect of WNT10B on normal rat prostate development, rudimentary VP lobes were harvested on pnd1 and contralateral lobes cultured for 4 days in either basic organ culture medium (BOCM: DMEM/F12 [Invitrogen/Gibco, Carlsbad, CA], 50 μg/mL gentamycin, 1× insulin-transferrin-selenium, 10 nM testosterone [Sigma-Aldrich, St Louis, MO] with 0.5 μg/mL WNT10B protein (R&D Systems, Minneapolis, MN) or 0.5 μg/mL bovine serum albumin as control. Tissues were floated on Millicell-CM filters (Millipore Corp, Bedford, MA) in 2 mL medium in BD Falcon 12-well plates (BD Biosciences, San Jose, CA) in humidified culture chambers at 37°C, 5% CO_2 on an automated X-Y-Z stage attached to a Zeiss Axiovert 200 inverted microscope with an Axiocam HRm digital camera (Carl Zeiss Microscopy LLC, Thornwood, NY). Photographs were captured daily and media changed every 48 hours.

2.3 | Immunohistochemistry

Tissues were fixed in methacarn overnight and paraffin-embedded. Tissue sections were heat-treated for antigen retrieval in a Decloaker pressure cooker (Biocare Medical, Walnut Creek, CA) in Tris-EDTA, pH 9.0. Sections were blocked with SuperBlock (Thermo Fisher Scientific, Waltham, MA) and incubated overnight at 4°C with rabbit anti-WNT10B antibody (1:200; Santa Cruz Biotechnology, Santa Cruz, CA), guinea pig anti-CK8/18 (1:800; American Research Products 03-GP11, Belmont, MA) or rabbit anti-Ki67 (1:200; Abcam, Cambridge, MA). The sections were reacted with biotinylated anti-IgG (Vector Laboratories, Inc) and detected with avidin-biotin peroxidase (ABC-Elite, Vector Laboratories, Burlingame, CA) using diaminobenzidine tetrachloride (DAB) as chromagen. For controls, normal rabbit, or guinea pig IgG was substituted for primary antibody. The sections were counterstained with Gill's #3 hematoxylin (1:4).

2.4 | PCa TMA and analysis

PCa progression TMA slides were obtained from the Cooperative Human Tissue Network, Mid-Atlantic Division and immunostained for WNT10B. TMA was reviewed for Gleason

grade and scored by two board-certified pathologists from the University of Illinois Department of Pathology. The TMA slide was scanned at ×20 magnification on a Leica Aperio AT2 slide scanner (Leica Biosystems Imaging, Inc, Vista, CA). The image was loaded into Indica Labs Halo v 2.3.2089 and segmented into TMA spots. The Halo AI module was used to create a tissue classifier with epithelium and stroma classes. The levels of WNT10B protein stain were quantified within the epithelium class using the multiplex immunohistochemistry (IHC) v 2.0.3 algorithm. Nuclei were segmented using hematoxylin and DAB signals and estimated cytoplasm objects were grown around the nuclei. Thresholds were set for cytoplasmic positivity and per cell data were exported. The same thresholds were used for every TMA spot. Cytoplasmic percent positivity and average intensity of *WNT10B* staining in the cytoplasm were exported for each spot. Data per spot were combined using software R Studio 1.1.442 and R version 3.4.1.

2.5 | Cell culture

PC3 cells, a metastatic PCa cell line, were obtained from ATCC (Manassas, VA) and PC3M cells, a more aggressive PC3 derivative were obtained from Dr Jindan Yu, Northwestern University, Chicago, IL. Both were cultured in RPMI-1640 medium supplemented with 10% fetal bovine serum (FBS), and 1% penicillin/streptomycin. HuSLC, a gift from Dr Susan Kasper, University of Cincinnati, Cincinnati, OH were cultured under embryonic stem cell (ESC) conditions using defined ESC medium (DMEM/F12, KnockOut Serum Replacement [Invitrogen/Gibco] and 4 ng/mL recombinant bFGF [Gibco]) on Matrigel-coated (BD Biosciences, Bedford, MA) plates. HuSLC passage 38 cells were thawed and passaged less than five times for the duration of this study. All cells were cultured at 37°C, 5% CO_2, and passaged at subconfluence.

2.6 | Stable knockdown in PC3

WNT10B short hairpin RNA (shRNA) and control shRNA lentiviral constructs were purchased from Santa Cruz Biotechnology (Santa Cruz, CA). *WNT10B* shRNA lentivirus or control shRNA lentivirus was added to appropriate wells with consequent puromycin selection at 1.0 μg/mL for a minimum of three passages and then maintained in puromycin for remainder of studies. A minimum of three PC3 *WNT10B* knockdown and control batches were created and *WNT10B* mRNA knockdown was confirmed by quantitative reverse transcription polymerase chain reaction (qRT-PCR).

2.7 | Cell proliferation assay

A 3-(4,5-dimethylthiazol-2-yl)-2,5-diphenyltetrazolium bromide (MTT; Invitrogen) assay was performed according to manufacturer's instructions at 24, 48, and 72 hours post seeding with a minimum of five wells per time point. On the day of harvest, fresh medium was replaced before addition of MTT. Cells were incubated at 37°C for 4 hours, medium was removed, dimethyl sulfoxide added and incubated for 10 minutes. Each sample was mixed and absorbance read at 540 nm using a BioTek reader.

2.8 | Scratch assay

PC3 cells were grown to confluence in 12-well plates in complete medium. Following scratch through the cultured cells, images captured at 0, 24, 48, and 72 hours. The percentage of scratch not covered at each time point was quantified using Axiovision software.

2.9 | Side population analysis for stem cell-like populations

Control shRNA-PC3 cells and *WNT10B* shRNA-PC3 cells were cultured to subconfluence and trypsinized. Cells were resuspended in Hank's balanced salt solution (HBSS; 10% FBS, 20 mM 4-(2-hydroxyethyl)-1-piperazineethanesulfonic acid, 1% D-glucose) and stained with 5 μg/mL Hoechst 33342 ± 50 μM verapamil for 60 minutes at 37°C. Cells were washed and resuspended in ice-cold Hoechst buffer containing 1 μg/mL propidium iodide for dead cell discrimination immediately before fluorescence-activated cell sorting (FACS) analysis. Flow cytometry was carried out using a Beckman Coulter MoFlo Flow Cytometer.

2.10 | Real-time PCR

Total RNA was extracted using RNeasy Kit (Qiagen, Valencia, CA) with on-column DNase I digestion. RNA was reverse-transcribed with RNase H+ MMLV reverse transcriptase at 42°C for 30 minutes using an iScript cDNA Synthesis Kit (Bio-Rad, Hercules, CA). A blend of oligo(dT) and random primers were used for reverse transcription. Real-time PCR in SsoAdvanced SYBR Green Master Mix (Bio-Rad) was carried out using CFX96 Touch Real-time PCR Detection System (Bio-Rad). Primer sequences are listed in Table S1. Cycling conditions were 95°C for 3 minutes, 40 cycles of 95°C for 15 seconds, and 60°C for 30 seconds. Optical data obtained by real-time PCR were analyzed with the manufacturer's software (CFX96 Manager Software ver. 3.0). Data were analyzed by $\Delta\Delta C_T$ method. mRNA levels for each gene were normalized to house-keeping gene ribosomal protein L13 (Rpl13). Each assay was independently repeated a minimum of three times.

2.11 | PCR array

VP *Wnt* gene expression from WT and SV40/Pb rats was screened using the rat Wnt RT^2 Prolifer PCR Array System (SuperArray Bioscience, Frederick, MD) following manufacturer's instructions. Total RNA was extracted from pulverized prostate tissue using RNeasy Kit and complementary DNA was generated as described above. Arrays were run on a QuantStudio6 (Thermo Fisher Scientific) and normalized independently using five reference genes according to the manufacture's protocol. The $\Delta\Delta C_T$ method was used for comparative analysis.[24] Arrays were repeated three times for each rat genotype.

2.12 | RNA-Seq data set

RNA-seq data from Stand Up to Cancer and Johns Hopkins University were analyzed as previously described.[25] Raw RNA-Seq FASTQ data files were obtained on 25 prostate tumors and 51 annotated metastases via dbGAP (phs000310.v1.p1 for tumors and benign glands; phs000915.v1.p1 for metastases[26,27]). These data sets were chosen based upon the quality of mRNA, sequencing depth, and annotation. The tumor data sets were from patients who had undergone prostatectomy without prior therapy whereas the metastases were from

patients with castration-resistant PCa, some of which had received taxane, enzalutamide, or abiraterone treatment.[26,27] The quality of raw reads was accessed by FastQC (v0.11.4). All reads were mapped to the human genome assembly (NCBI build 19) using STAR (v2.5.1b). Alignment metrics were collected by Picard tools (v2.8.1) and RSeQC (v2.6.4[27]). Transcripts were assembled from the aligned reads using Cufflinks and combined with known gene annotation. The expression level of transcripts was quantified using FPKM fragments per kilobase of transcript per million mapped reads (FPKM)-based and read count-based methods. Transcript expression was normalized across samples.

2.13 | Statistical analysis

Data were analyzed using Instat ver. 3 (GraphPad Software, Inc, San Diego, CA) using Students' *t* test or analysis of variance as appropriate, followed by posthoc tests. Values are expressed as mean ± SEM, and $p < .05$ was considered significant.

3 | RESULTS

3.1 | Ontogeny and role of WNT10B in the developing rat prostate gland

The temporal and spatial expression pattern of *Wnt10b* was followed in the ventral lobe of the developing rat prostate through adulthood. Expression levels of *Wnt10b* mRNA were high in the pnd1 rudimentary prostate and dropped precipitously as branching morphogenesis commenced, reaching a nadir by pnd3 which was sustained through adulthood (Figure 1A). Published work by others has shown *Wnt10b* message localization to the urogenital epithelium in the developing murine prostate.[6] We confirmed this in the rat prostate using IHC for WNT10B protein which localized to the epithelium (Figure 1B), similar to the lung bronchus as a positive control (Figure S1). An organ culture system that recapitulates prostate morphogenesis was used to examine the effects of WNT10B protein on prostate growth. While culture of newborn rat VPs for 4 days in testosterone resulted in morphogenesis of a complex branched ductal structure, addition of 0.5 μg/mL WNT10B markedly inhibited ductal outgrowth and branching (Figure 1C and 1D). Together, these results suggest that WNT10B has a growth-suppressive role in the prostate and reduced expression is essential for branching morphogenesis.

3.2 | WNT10B expression in localized PCa

The growth-suppressive effect of WNT10B, as well as other WNTs,[28,29] on the developing rat prostate raises the possibility that dysregulated expression of *Wnt* genes might contribute to aberrant growth in PCa. To examine this directly, we utilized the rat probasin/TAg PCa model which develops prostate epithelial neoplasia (PIN) by 5 weeks, carcinomas at 100% incidence by 15 weeks and at 25 weeks, the histological grade of prostate tumors ranges from well-differentiated to poorly differentiated adenocarcinomas with lesions resembling the human disease.[23] Expression of *Wnt* genes was interrogated in VPs of 25-week-old probasin/TAg rats and WT controls using rat *Wnt* PCR arrays. While consistent downregulation of most *Wnt* genes was observed in the probasin/Tag tumors compared with WT prostates, only *Wnt*1, *Wnt10b*, *Wnt* 5a, and *Wnt* 11 were statistically significant (Figure 2A). Importantly, *Wnt10b* expression showed a 25-fold decrease in PCa compared with WT prostates, by far the greatest *Wnt* expression loss. Histologically, poorly differentiated

adenocarcinoma was found throughout the VPs of the probasin/TAg rats with markedly increased proliferation (Ki67+) and loss of WNT10B at the protein level as compared with WT prostates (Figure 2B).

To investigate whether loss of Wnt10b expression in the rat model of localized PCa is observed in humans, WNT10B protein levels were examined in a human localized PCa progression tissue microarray (TMA; Figure 3A). Interestingly, the percentage of WNT10B-expressing cells was increased in PIN compared with normal epithelial cells but then subsequently decreased as localized PCa developed with significantly lower levels noted in Gleason grade 10 tumors (Figure 3B). Similar findings were noted for WNT10B protein intensity within the specimens (Figure 3C). Together, these results implicate a potential involvement of reduced WNT10B actions in localized PCa progression in both rat and human disease.

3.3 | The role of WNT10B in PCa metastatic progression

We next undertook a series of experiments to examine whether WNT10B may play a role in PCa metastatic progression. First, *WNT10B* mRNA expression was evaluated in three PCa cell lines and primary cultures of nondiseased prostate epithelial cells (PrEC). Relative to PrEC, *WNT10B* mRNA was significantly increased in HuSLC, a spontaneously immortalized PCa stem-like cell line from a Gleason grade 9 tumor[30] (Figure 4A). While the androgen-independent metastatic PC3 cells expressed similar *WNT10B* as HuSLCs, a more aggressive variant, PC3M[31] expressed higher levels of *WNT10B* than the parental PC3 line. To investigate clinical relevance, we queried an RNA-seq database of highly annotated localized PCa and metastatic castrate-resistant PCa specimens for *WNT10B* expression.[25] Similar to the metastatic cell lines, there was a significant increase in *WNT10B* mRNA in the metastatic specimens compared with the localized PCas (Figure 4B). Furthermore, in metastatic castrate-resistant PCa specimens, there was a reduction in *WNT10B* expression following treatment with enzalutamide, abiraterone, or taxanes.

To interrogate whether WNT10B has antiproliferative effects in metastatic PCa, *WNT10B* was stably knocked down in PC3 cells using an shRNA lentivirus with *WNT10B* knockdown confirmed via RT-PCR (Figure S2). Using an MTT assay, PC3 cells with stable knockdown of *WNT10B* showed a significant increase in proliferation at 24 hours that was double the control shRNA by 48 hours (Figure 5A). Next, a scratch assay using shRNA *WNT10B* PC3 cells revealed complete wound healing at 48 hours with *WNT10B* knockdown compared with partial closure with control shRNA, indicative of increased proliferation upon *WNT10B* silencing (Figure 5B). To examine whether *WNT10B* gene knockdown could alter in vivo tumor burden, the stable shRNA *WNT10B* PC3 cells or shRNA scramble control cells (10^6 cells per site) were inoculated s.c. in nude mice. At 30 days, s.c. tumors of Sh*WNT10B*-PC3 cells were significantly larger than the control PC3 cells, confirming an in vivo antiproliferative role of *WNT10B* in the metastatic PC3 cell line (Figure 5C). Together, these findings support a continued role for *WNT10B* in reducing metastatic PCa proliferation both in vitro and in vivo.

Since *WNT10B* expression was elevated in the cancer stem-like cells, HuSLC, and increased from primary to metastatic PCa, we tested whether WNT10B's role in advanced disease

may involve reversion to the early embryonic role of WNT10B which includes regulation of stemness. As acquisition of stemness characteristics in cancer cells co-occurs with epithelial to mesenchymal transition (EMT) and invasion, we first examined EMT and metalloproteinase (MMP) genes. ShRNA knockdown of *WNT*10B in PC3 cells reversed the EMT signature as seen by elevated epithelial E-cadherin, and reduced mesenchymal vimentin and N-cadherin expression as compared with control shRNA-PC3 cells (Figure 6A). While expression of matrix metalloprotease genes MMP2 was modestly reduced, knockdown of *WNT10B* in PC3 cells resulted in a marked suppression of MMP9 expression (Figure 6A). Together, these results suggest that *WNT*10B may contribute to the invasive potential of PC3 cells. Importantly, knockdown of *WNT10B* resulted in a marked decrease in NANOG and SOX2 expression, two bonafide stemness genes suggesting continued control of stemness potential in this metastatic cell line (Figure 6A). To directly assess the effect of loss of *WNT10B* on PC3 stem-like cells, a Hoechst dye exclusion assay was used to assess the stem cell-like side population. FACS results revealed that *WNT10B* knockdown significantly reduced this population compared with shRNA control cells, indicating that loss of *WNT10B* largely eliminates the PCa stem-like cells within cultured PC3 cells (Figure 6B).

Understanding that there is known crosstalk between WNT signaling and various other signaling effectors, we investigated whether knockdown of *WNT10B* specifically could be affecting one such effector, transforming growth factor β1 (TGFβ1), which plays roles in both local and advanced PCa. TGFβ1 levels were reduced following knockdown of *WNT10B* in PC3 cells suggesting crosstalk between the two genes (Figure S3).

To assess whether the reduction in EMT properties and stem cell numbers with *WNT10B* gene knockdown could influence the tumor metastatic potential, primary tumors from the stable shRNA *WNT10B* PC3 cells or shRNA scramble control cells (Figure 5C) were serially transplanted into new host nude mice. Strikingly, knockdown of *WNT10B* totally abrogated the ability of PC3 primary tumors to propagate new tumors either s.c. or under the renal capsule of host mice (Figure 7A). Furthermore, while evidence of lung metastasis was evident in the lungs of host mice harboring the PC3 control shRNA tumor transplants, no distant metastases were found in mice with *WNT10B* shRNA tumors, documenting in vivo loss of metastatic potential following *WNT10B* knockdown (Figure 7B).

4 | DISCUSSION

This study identifies important roles for canonical WNT10B in prostate gland development as well as in PCa growth and progression. Previous studies have localized *Wnt10b* mRNA to the epithelium of nascent buds of the mouse prostate during early development[6,20] and we herein confirm that WNT10B protein is similarly localized to the developing rat prostate epithelium. This localization pattern is similar to dental epithelium and mammary epithelial placodes[32] but contrasts with stromal *Wnt10b* expression in other systems including fetal bone stromal cells[33] and stromal vascular cells of adipose tissue,[34] highlighting the organ-specific differences in expression. That WNT10B protein is not observed in the prostate stromal compartment indicates an autocrine or epithelial-only paracrine function for this morphogen. The ontogeny of *Wnt10b* followed a similar profile to previously published

Wnt5a[35] and *Wnt2*[29] ontogeny in the developing rat prostate with rapid decline to a nadir postnatally concomitant with ductal elongation and extensive branching suggesting that their rapid loss may be necessary for controlled prostate growth. Indeed, direct evidence for this comes from ex vivo analysis with neonatal rat prostates where exogenous WNT10B protein inhibited ductal outgrowth and branching indicating an antiproliferative role for WNT10B on prostate epithelium. *Wnt10b* is the first *Wnt* ligand expressed in the murine prostate anlage at the time of initial budding,[20] which implicates a potential function in prostate determination. A critical role for *WNT10B* in directing prostatic fate was directly supported by our previous work that showed *WNT10B* was essential for in vitro directed differentiation of hESCs into prostatic organoids, an effect that could not be replicated with canonical WNT3A.[22] More recently, human prostate stem cells isolated from disease-free primary specimens showed specific immunostaining for WNT10B while daughter progenitor cells were largely negative[36] which suggests a continued function for WNT10B in stem cell maintenance in the adult prostate. Implicated roles for WNT10B in regulating stemness have been reported in other organ systems including hematopoietic stem cells where WNT10B was shown to promote in vitro proliferation.[33] In contrast, *WNT10B* expression inhibited the in vitro proliferation of erythroid progenitor cells underscoring the difference in activity of this ligand depending on cellular context.[33]

Since growth and progression of PCa have previously been linked to developmental signals gone awry,[7–9] we herein investigated whether the antiproliferative and prostemness roles for WNT10B during development might be co-opted in a manner that promotes PCa growth and/or progression including metastasis. Indeed, in the probasin/TAg rat prostate adenocarcinoma model, *Wnt10b* expression was reduced over 25-fold while WNT10B protein was lost in the tumors concomitant with hyperproliferation at those sites which suggest that loss of WNT10B and its antiproliferative effects may contribute to uncontrolled growth of the cancerous cells. Investigation of organ-confined human PCa progression TMAs revealed a slightly different story but overall similar premise. Compared with normal prostate epithelium, WNT10B protein increased in PIN lesions when transformative events occur but then decreased with PCa progression, reaching the lowest levels in the most aggressive Gleason scores 8 to 10 specimens which may permit a proproliferative state that contributes to local progression. These findings are consistent with other reports that show an antiproliferative effect for WNT10B with overexpression in Huh-7 hepatocellular carcinoma cells resulting in reduced growth rate in monolayer culture and on agar plates.[37]

To interrogate the roles of WNT10B in PCa progression, we examined two metastatic cell lines, PC3 and its more aggressive variant PC3M, as well as a spontaneously immortalized cancer stem-like cell line, HuSLC, from a Gleason 9 localized PCa. Surprisingly, compared with disease-free PrEC cells, *WNT10B* message levels in HuSLC, PC3 and cells were markedly elevated with the more aggressive PC3M variant expressing double the *WNT10B* levels as the parental line. Similarly, RNA sequencing data from human localized and metastatic PCa revealed that compared with prostatectomy specimens, the metastatic specimens had significantly higher expression of *WNT10B*. Furthermore, of the metastatic specimens, some of which were treated with enzalutamide, abiraterone, or taxane, there was a decrease in *WNT10B* expression posttreatment thus indirectly implicating a role for

WNT10B in promoting metastatic disease. Together, these data suggest that *WNT10B* may have different roles in PCa based on disease stage.

Since the cancer stem-like HuSLC cells had robust *WNT10B* expression, we asked whether increased *WNT10B* re-expression in late stage disease might promote stem-like properties in the tumors that enable EMT and tumor repopulation. Indeed, experiments to directly test this using *WNT10B* silencing support this premise. While stable knockdown of *WNT10B* in PC3 identified a continued antiproliferative role by MTT and scratch assays, new actions that promote PCa progression were revealed. Specifically, EMT was reversed, MMP9 expression declined, stemness gene expression was reduced and stem-like cell numbers in PC3 cultures plummeted. This ultimately presents a profile of decreased aggressive capacity in PC3 cells when the elevated WNT10B levels seen in metastatic cells are reduced. Inasmuch as the mechanism of EMT is still contested, there is more agreement that it is a necessary process to promote metastasis and this ability is likely conferred by stem-like properties in a subset of cancer cells.[38–40] This prostemness role for WNT10B is consistent with WNT10B's role in other organ systems including adipose progenitors and hematopoietic stem cells.[33,41] Most importantly, when elevated levels of *WNT10B* in PC3 cells were reduced by shRNA, although they were able to form larger initial tumors due to increased proliferative capacity, the capability for in vivo tumor repopulation and metastasis were eliminated upon serial transplantation. These results present direct in vivo evidence for the critical role of *WNT10B* in maintaining stemness in late-stage PCa disease which is essential for tumor metastasis.

The switch of WNT10B from a tumor suppressor in localized disease to a metastasis promoter in PCa progression underscores and suggests possible functional exchanges between other signaling effectors. Notably, there is precedence for this concept of differential gene regulation based on tumor stage including TGFβ1 in breast carcinoma and ERβ in PCa where expression of both genes are decreased in early stages of their respective diseases but are re-expressed at high levels at the advanced disease stage.[42,43] We investigated the levels of *TGFβ1* following *WNT10B* knockdown and found them to be significantly reduced (Figure S3). TGFβ1 in normal conditions inhibits cell growth, promotes differentiation, and induces apoptosis.[44–46] Further, TGFβ1 and canonical WNT signaling have been reported to stimulate each other through Smad and non-Smad pathways.[47] As such, the loss of the antiproliferative WNT10B effects in localized PCa may be, in part, mediated through downregulation of TGFβ1. However, TGFβ1 is also known to be a primary inducer of EMT[48] which underscores its role as a driver of aggressive disease.[49] In this context, reversion of the EMT phenotype and aggressive characteristics seen with knockdown of WNT10B could similarly be mediated through downregulation of TGFβ1. Obviously, this poses a conundrum with targeted therapy as stage of disease becomes critically important with the risk of TGFβ1 downregulation inhibiting metastatic disease progression while concomitantly leading to a loss of tumor suppression in a different subset of cells. In summary, this study establishes a role for WNT10B in prostate gland development and PCa progression which is schematized in Figure 8. Early expression of *WNT10B* in prostate epithelium is implicated in the determination of undifferentiated UGE and stem cell lineage commitment while a rapid decrease to nadir levels is necessary to restrain its antiproliferative actions and permit glandular morphogenesis and homeostasis

through adulthood. In localized PCa, high levels of WNT10B are noted in PIN during initial transformation whereas decreased *WNT10B* expression upon cancer development permits a hyperproliferative state conducive for tumor formation. As the disease progresses, elevated *WNT10B* expression is involved in driving a cancer stem cell phenotype with increased EMT and invasive capacity. In this context of advanced disease, loss of WNT10B results in a reduction of stemness potential, a reversal of EMT, and ultimately an inability to metastatically propagate tumor growth. These findings present WNT10B as a novel therapeutic target for advanced, androgen-independent PCa with the goal of eliminating metastatic disease.

Supplementary Material

Refer to Web version on PubMed Central for supplementary material.

ACKNOWLEDGMENT

This study was supported in part by NIH training grant T32DK007739, NIH/NIDDK R01 DK40890, NIH/NIEHS R01 ES015584 and the Michael Reese Research and Education Foundation. Histology/tissue microarray/imaging services were provided by the Research Resources Center-Research Histology and Tissue Imaging Core at the University of Illinois at Chicago established with the support of the Vice-Chancellor of Research. We wish to acknowledge and thank Dr Andre Kajdacsy-Balla and Dr Virilia Macias from UIC Department of Pathology for reviewing and scoring the prostate cancer TMA slides. We also wish to thank Lynn Birch for help with animal breeding and manuscript preparation, Dr Susan Kasper at the University of Cincinnati for the gift of HuSLC cells and Dr Jindan Yu at Northwestern University for the gift of PC3M cells.

REFERENCES

1. Timms BG, Mohs TJ, Didio LJA. Ductal budding and branching patterns in the developing prostate. J Urol. 1994;151(5):1427–1432. [PubMed: 8158800]
2. Prins GS, Putz O. Molecular signaling pathways that regulate prostate gland development. Differentiation. 2008;76(6):641–659. [PubMed: 18462433]
3. Bieberich CJ, Fujita K, He WW, Jay G. Prostate-specific and androgen-dependent expression of a novel homeobox gene. J Biol Chem. 1996;271(50):31779–31782. [PubMed: 8943214]
4. Bhatia-Gaur R, Donjacour AA, Sciavolino PJ, et al. Roles for Nkx3.1 in prostate development and cancer. Genes Dev. 1999;13(8):966–977. [PubMed: 10215624]
5. Gao H, Ouyang X, Banach-Petrosky WA, Shen MM, Abate-Shen C. Emergence of androgen independence at early stages of prostate cancer progression in Nkx3.1; Pten mice. Cancer Res. 2006;66(16):7929–7933. [PubMed: 16912166]
6. Mehta V, Abler LL, Keil KP, Schmitz CT, Joshi PS, Vezina CM. Atlas of Wnt and R-spondin gene expression in the developing male mouse lower urogenital tract. Dev Dyn. 2011;240(11):2548–2560. [PubMed: 21936019]
7. McNeal JE. Origin and evolution of benign prostatic enlargement. Invest Urol. 1978;15(4):340–345. [PubMed: 75197]
8. Shaw A, Gipp J, Bushman W. The sonic Hedgehog pathway stimulates prostate tumor growth by paracrine signaling and recapitulates embryonic gene expression in tumor myofibroblasts. Oncogene. 2009;28(50):4480–4490. [PubMed: 19784071]
9. Murillo-Garzón V, Kypta R. WNT signalling in prostate cancer. Nat Rev Urol. 2017;14(11):683–696. [PubMed: 28895566]
10. Potter SR, Partin AW. Prostate cancer: detection, staging, and treatment of localized disease. Semin Roentgenol. 1999;34(4):269–283. [PubMed: 10553603]
11. Westover K, Chen MH, Moul J, et al. Radical prostatectomy vs radiation therapy and androgen-suppression therapy in high-risk prostate cancer. BJU Int. 2012;110(8):1116–1121. [PubMed: 22540922]

12. Taplin ME, Balk SP. Androgen receptor: a key molecule in the progression of prostate cancer to hormone independence. J Cell Biochem. 2004;91(3):483–490. [PubMed: 14755679]
13. Xin L, Lawson DA, Witte ON. The Sca-1 cell surface marker enriches for a prostate-regenerating cell subpopulation that can initiate prostate tumorigenesis. Proc Natl Acad Sci USA. 2005;102(19):6942–6947. [PubMed: 15860580]
14. Wang X, Julio MK, Economides KD, et al. A luminal epithelial stem cell that is a cell of origin for prostate cancer. Nature. 2009;461(7263):495–500. [PubMed: 19741607]
15. Bisson I, Prowse DM. WNT signaling regulates self-renewal and differentiation of prostate cancer cells with stem cell characteristics. Cell Res. 2009;19(6):683–697. [PubMed: 19365403]
16. Ishikawa T, Tamai Y, Zorn AM, et al. Mouse Wnt receptor gene Fzd5 is essential for yolk sac and placental angiogenesis. Development. 2001;128(1):25–33. [PubMed: 11092808]
17. Kemp C, Willems E, Abdo S, Lambiv L, Leyns L. Expression of all Wnt genes and their secreted antagonists during mouse blastocyst and postimplantation development. Dev Dyn. 2005;233(3):1064–1075. [PubMed: 15880404]
18. Liu X, Mazanek P, Dam V, et al. Deregulated Wnt/β-catenin program in high-risk neuroblastomas without MYCN amplification. Oncogene. 2008;27(10):1478–1488. [PubMed: 17724465]
19. Bui TD, Rankin J, Smith K, et al. A novel human Wnt gene, WNT10B, maps to 12q13 and is expressed in human breast carcinomas. Oncogene. 1997;14(10):1249–1253. [PubMed: 9121776]
20. Abler LL, Keil KP, Mehta V, Joshi PS, Schmitz CT, Vezina CM. A high-resolution molecular atlas of the fetal mouse lower urogenital tract. Dev Dyn. 2011;240(10):2364–2377. [PubMed: 21905163]
21. Pu Y, Huang L, Prins GS. Sonic hedgehog-patched Gli signaling in the developing rat prostate gland: lobe-specific suppression by neonatal estrogens reduces ductal growth and branching. Dev Biol. 2004;273(2):257–275. [PubMed: 15328011]
22. Calderon-Gierszal EL, Prins GS. Directed differentiation of human embryonic stem cells into prostate organoids in vitro and its perturbation by low-dose bisphenol A exposure. PLOS One. 2015;10(7):e0133238. [PubMed: 26222054]
23. Asamoto M, Hokaiwado N, Cho YM, et al. Prostate carcinomas developing in transgenic rats with SV40 T antigen expression under probasin promoter control are strictly androgen dependent. Cancer Res. 2001;61(12):4693–4700. [PubMed: 11406539]
24. Livak KJ, Schmittgen TD. Analysis of relative gene expression data using real-time quantitative PCR and the 2−ΔΔCT method. Methods. 2001;25(4):402–408. [PubMed: 11846609]
25. Bhanvadia RR, VanOpstall C, Brechka H, et al. MEIS1 and MEIS2 expression and prostate cancer progression: a role for HOXB13 binding partners in metastatic disease. Clin Cancer Res. 2018;24(15):3668–3680. [PubMed: 29716922]
26. Pflueger D, Terry S, Sboner A, et al. Discovery of non-ETS gene fusions in human prostate cancer using next-generation RNA sequencing. Genome Res. 2011;21(1):56–67. [PubMed: 21036922]
27. Robinson D, Van Allen EM, Wu YM, et al. Integrative clinical genomics of advanced prostate cancer. Cell. 2015;161(5):1215–1228. [PubMed: 26000489]
28. Huang L, Xiao A, Choi SY, et al. Wnt5a is necessary for normal kidney development in zebrafish and mice. Nephron Exp Nephrol. 2014;128(1–2):80–88. [PubMed: 25412793]
29. Madueke IC, Hu WY, Huang L, Prins GS. WNT2 is necessary for normal prostate gland cyto-differentiation and modulates prostate growth in an FGF10 dependent manner. Am J Clin Exp Urol. 2018;6(4):154–163. [PubMed: 30246051]
30. Vummidi Giridhar P, Williams K, VonHandorf AP, Deford PL, Kasper S. Constant degradation of the androgen receptor by MDM2 conserves prostate cancer stem cell integrity. Cancer Res. 2019;79(6):1124–1137. [PubMed: 30626627]
31. Kozlowski JM, Fidler IJ, Campbell D, Xu ZL, Kaighn ME, Hart IR. Metastatic behavior of human tumor cell lines grown in the nude mouse. Cancer Res. 1984;44(8):3522–3529. [PubMed: 6744277]
32. Veltmaat JM, Van Veelen W, Thiery JP, Bellusci S. Identification of the mammary line in mouse by Wnt10b expression. Dev Dyn. 2004;229(2):349–356. [PubMed: 14745960]
33. Van Den Berg DJ, Sharma AK, Bruno E, Hoffman R. Role of members of the Wnt gene family in human hematopoiesis. Blood. 1998;92(9):3189–3202. [PubMed: 9787155]

34. Bennett CN, Ross SE, Longo KA, et al. Regulation of Wnt signaling during adipogenesis. J Biol Chem. 2002;277(34):30998–31004. [PubMed: 12055200]
35. Huang L, Pu Y, Hu WY, et al. The role of Wnt5a in prostate gland development. Dev Biol. 2009;328(2):188–199. [PubMed: 19389372]
36. Hu WY, Hu DP, Xie L, et al. Isolation and functional interrogation of adult human prostate epithelial stem cells at single cell resolution. Stem Cell Res. 2017;23:1–12. [PubMed: 28651114]
37. Yoshikawa H, Matsubara K, Zhou X, et al. WNT10B functional dualism: β-catenin/Tcf-dependent growth promotion or independent suppression with deregulated expression in cancer. Mol Biol Cell. 2007;18(11):4292–4303. [PubMed: 17761539]
38. Hay ED. An overview of epithelio-mesenchymal transformation. Acta Anat. 1995;154(1):8–20. [PubMed: 8714286]
39. Onder TT, Gupta PB, Mani SA, Yang J, Lander ES, Weinberg RA. Loss of E-cadherin promotes metastasis via multiple downstream transcriptional pathways. Cancer Res. 2008;68(10):3645–3654. [PubMed: 18483246]
40. Nakajima S, Doi R, Toyoda E, et al. N-cadherin expression and epithelial-mesenchymal transition in pancreatic carcinoma. Clin Cancer Res. 2004;10(12 Pt 1):4125–4133. [PubMed: 15217949]
41. Longo KA, Wright WS, Kang S, et al. Wnt10b inhibits development of white and brown adipose tissues. J Biol Chem. 2004;279(34):35503–35509. [PubMed: 15190075]
42. Reiss M, Barcellos-Hoff MH. Transforming growth factor-β in breast cancer: a working hypothesis. Breast Cancer Res Treat. 1997;45(1):81–95. [PubMed: 9285120]
43. Zhu X, Leav I, Leung YK, et al. Dynamic regulation of estrogen receptor-β expression by DNA methylation during prostate cancer development and metastasis. Am J Pathol. 2004;164(6):2003–2012. [PubMed: 15161636]
44. Chipuk JE, Bhat M, Hsing AY, Ma J, Danielpour D. Bcl-xL blocks transforming growth factor-β1-induced apoptosis by inhibiting cytochromec release and not by directly antagonizing Apaf-1-dependent caspase activation in prostate epithelial cells. J Biol Chem. 2001;276(28):26614–26621. [PubMed: 11320089]
45. El-Safadi M, Shinwari T, Al-Malki S, et al. Convergence of TGFβ and BMP signaling in regulating human bone marrow stromal cell differentiation. Sci Rep. 2019;9(1):4977. [PubMed: 30899078]
46. Kyprianou N, Isaacs JT. Expression of transforming growth factor-β in the rat ventral prostate during castration-induced programmed cell death. Mol Endocrinol. 1989;3(10):1515–1522. [PubMed: 2608047]
47. Vallée A, Lecarpentier Y, Guillevin R, Vallée JN. Interactions between TGF-β1, canonical WNT/β-catenin pathway and PPAR γ in radiation-induced fibrosis. Oncotarget. 2017;8(52):90579–90604. [PubMed: 29163854]
48. Wang Y, Zhou BP. Epithelial-mesenchymal transition in breast cancer progression and metastasis. Chin J Cancer. 2011;30(9):603–611. [PubMed: 21880181]
49. Dicken H, Hensley PJ, Kyprianou N. Prostate tumor neuroendocrine differentiation via EMT: the road less traveled. Asian J Urol. 2019;6(1):82–90. [PubMed: 30775251]

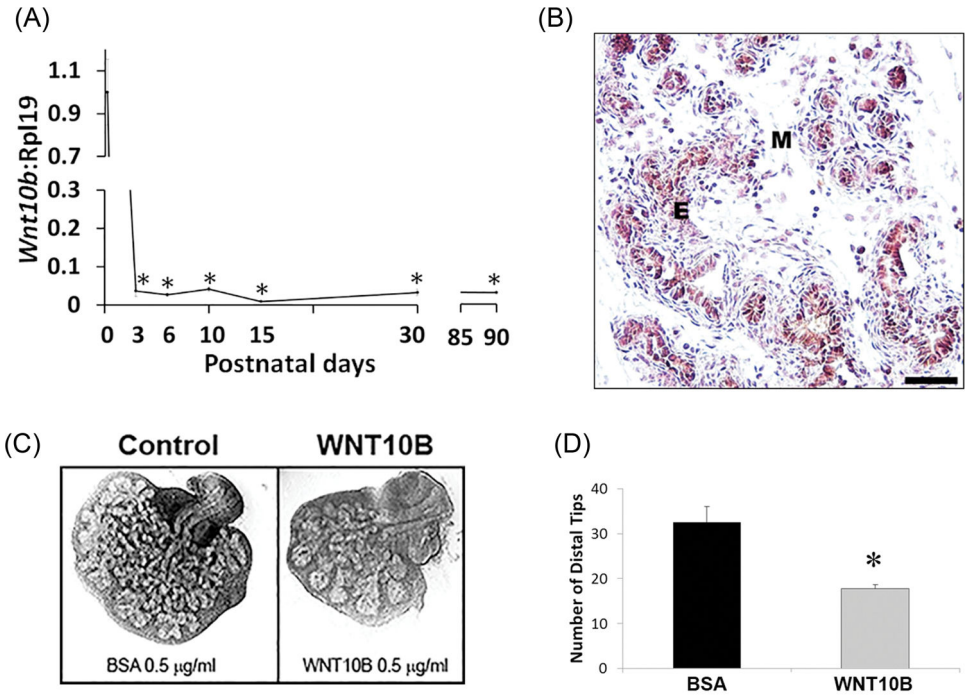

FIGURE 1.

A, Ontogeny of *Wnt10b* mRNA expression in the rat VP lobes as quantified by real-time reverse transcription PCR. *Wnt10b* expression was high at birth with a precipitous decline by pnd3 and maintained at nadir levels through adulthood. Each time point represents the mean ± SEM for 3 to 5 replicates. **P* < .001 vs pnd1. B, immunohistochemistry of pnd6 VP revealed WNT10B protein localization to epithelial (E) cells. (M) denotes mesenchyme. Scale bar = 50 μM. C, Paired neonatal VP lobes from a single rat were cultured in BSA (control) or WNT10B protein (0.5 μg/mL) for 4 days. WNT10B markedly reduced branching morphogenesis of the epithelium. D, VP distal tip number after 4 days of culture in BSA or WNT10B. Bars represent the mean ± SEM, *N* = 4, *P* < .05 vs BSA. BSA, bovine serum albumin; E, epithelial; M, mesenchyme; pnd, postnatal day; VP, ventral prostate

(A)

Group	Gene	p value	SV40/WT
Canonical Wnts	Wnt1	0.0186	-4.65
	Wnt2	0.3092	-2.22
	Wnt2b	0.5079	1.22
	Wnt3	0.1306	-2.27
	Wnt3a	0.0525	-2.73
	Wnt6	0.0806	-2.93
	Wnt7a	0.1306	-2.27
	Wnt7b	0.4532	1.37
	Wnt8a	0.1306	-2.27
	Wnt8b	0.1306	-2.27
	Wnt9a	0.0924	-2.43
	Wnt9b	0.1306	-2.27
	Wnt10a	0.1306	-2.27
	Wnt10b	0.0020	-25.11
Noncanonical Wnts	Wnt4	0.0811	-3.52
	Wnt5a	0.0429	-2.38
	Wnt5b	0.0821	-2.93
	Wnt11	0.0045	-2.49

(B)

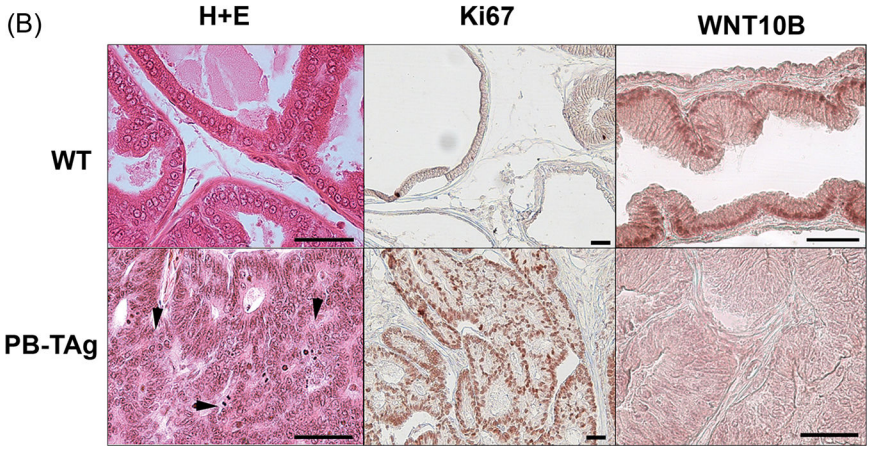

FIGURE 2.

A, Profile showing fold change in *Wnt* gene expression in probasin/TAg rat VPs at 25 weeks of age relative to WT prostates (SV40/WT) using a rat *Wnt* polymerase chain reaction array. Fold change in blue indicates a decrease and fold change in black is an increase relative expression levels. $N = 3$. B, Histology, Ki67 and WNT10B immunostaining in WT and probasin/Tag VPs at 25 weeks. (Top) WT VPs show normal glandular histology by hematoxylin and eosin stain, scarce proliferation by Ki67 labeling, and epithelial WNT10B immunostain. (Bottom) The probasin/Tag VP has widespread poorly differentiated adenocarcinoma (arrowheads), robust proliferation by Ki67 labeling, and marked reduction in epithelial WNT10B protein. Scale bar = 50 μM. VP, ventral prostate; WT, Wild type

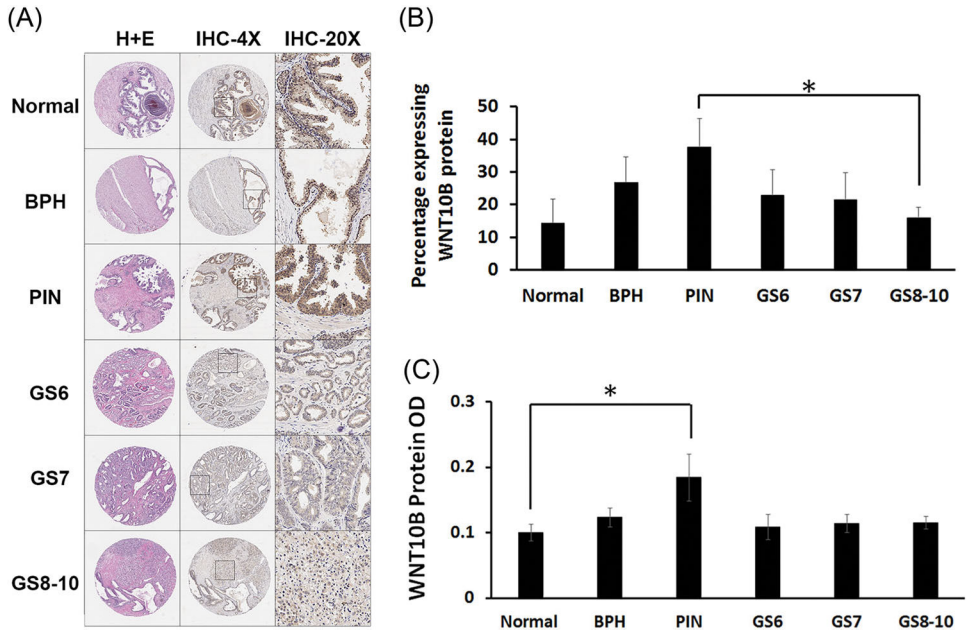

FIGURE 3.

WNT10B protein analysis in human PCa progression TMAs. A, TMAs stained with hematoxylin and eosin stain (first column) and immunostained for WNT10B at ×4 (second column) and ×20 magnification (third column). B, The total percentage of epithelial cells positive for WNT10B increased from normal prostate to BPH and PIN and then progressively decreased from PIN to PCa with increasing GS. **P* < .05 between PIN and GS 8 to 10. C, Average intensity of WNT10B protein immunostain was significantly increased from normal prostate to PIN (**P* < .05). Signal intensity was reduced with progression to PCa across the increasing GSs. Bars represent the mean ± SEM. N#: normal = 8, BPH = 9, PIN = 9; GS 6 = 8, GS 7 = 9, GS 8 to 10 = 10. BPH, benign prostatic hyperplasia; GS, Gleason score; PCa, prostate cancer; PIN, prostate intraepithelial neoplasia; TMA, tissue microarray

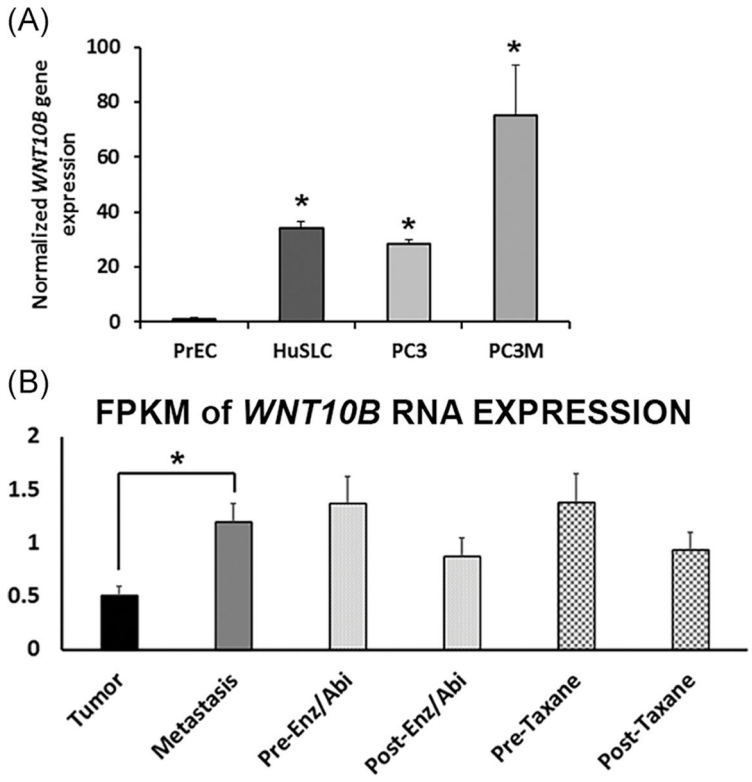

FIGURE 4.

WNT10B expression in PCa cell lines and patient specimens. A, Relative *WNT10B* expression in PrEC, HuSLC, PC3, and PC3M cells normalized to Rpl13a. *WNT10B* expression was significantly increased in all PCa cell lines relative to disease-free PrEC. $P <$ .005, $N = 3$. Bars represent the mean ± SEM. B, RNA-seq analysis of *WNT10B* expression in localized and metastatic human PCa specimens expressed as FPKM. *WNT10B* mRNA levels were significantly increased in metastatic PCa compared with localized PCa (*$P <$ .05). Metastatic samples were divided into pretreatment and posttreatment with Enz/Abi or taxane and *WNT10B* expression declined posttreatment in both groups, although this did not reach statistical significance. *$P <$ .05. Bars represent the mean ± SEM. Abi, abiraterone; Enz, enzalutamide; FPKM, fragments per kilobase of transcript per million; PCa, prostate cancer; PrEC, prostate epithelial cell

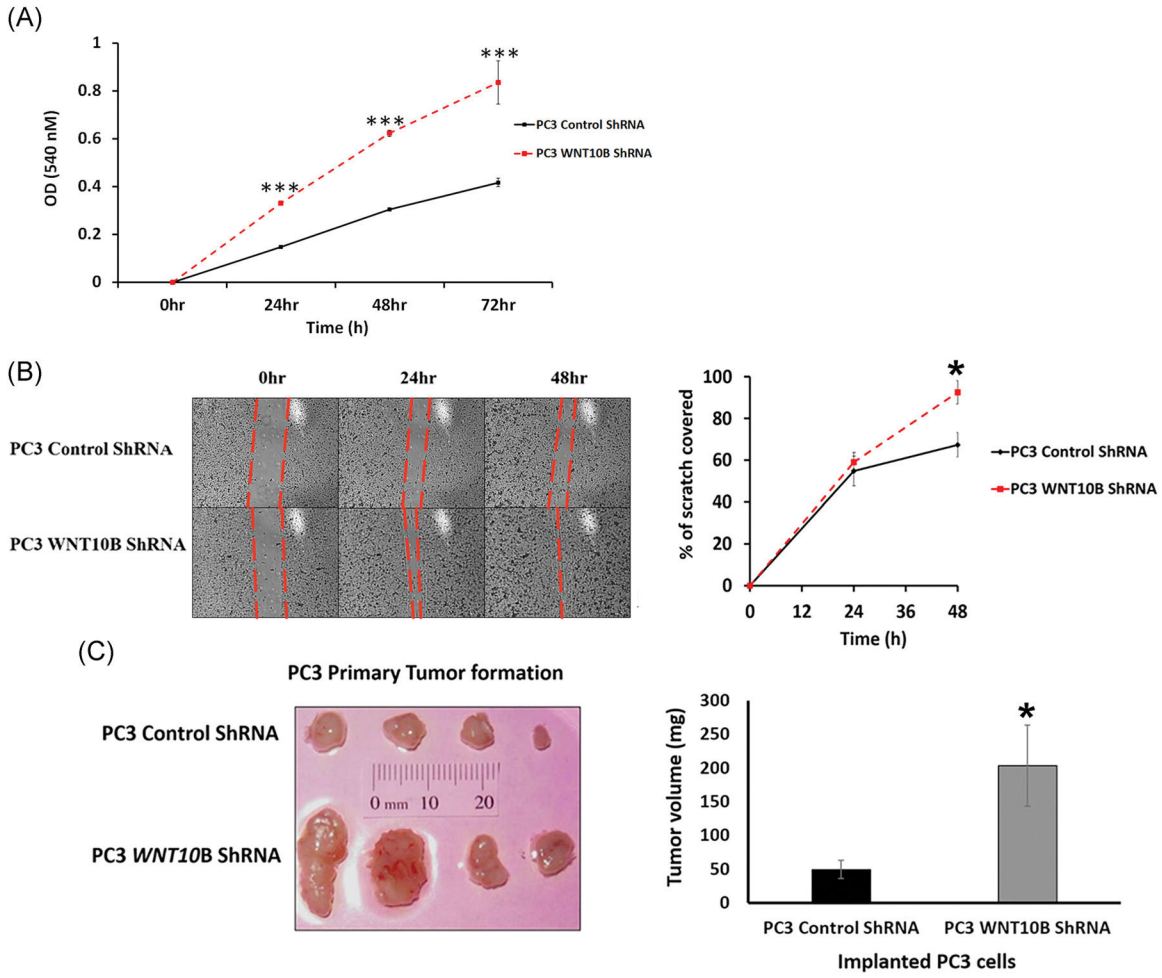

FIGURE 5.

Effect of *WNT10B* knockdown on PC3 cell in vitro and in vivo growth properties. A, Growth curves over 72 hours of PC3 shRNA control cells and PC3 *WNT10B* shRNA cells using an 3-(4,5-dimethylthiazol-2-yl)-2,5-diphenyltetrazolium bromide assay. Knockdown of *WNT10B* reduced cell growth in these metastatic cells. ***$P < .001$ vs PC3 control shRNA, $N = 5$. B, Cell migration activity was assessed in PC3 cells by a scratch assay. The percentage of scratch filled at 24 and 48 hours is shown graphically and documents that the migratory activity of PC3 cells was increased with *WNT10B* knockdown. *$P < .05$, $N = 3$, error bars represent SEM. C, Control shRNA and *WNT10B* shRNA-PC3 cells (1×10^6) were injected s.c. into the flanks of nude mice and resulting tumors grown for 30 days. The graph of tumor weights shows a significant increase in tumor size in the PC3 *WNT10B* shRNA cells compared with tumors generated by PC3 control shRNA cells. *$P < .05$ vs control PC3 cells. Bars represent the mean ± SEM. s.c., subcutaneously; shRNA, short hairpin

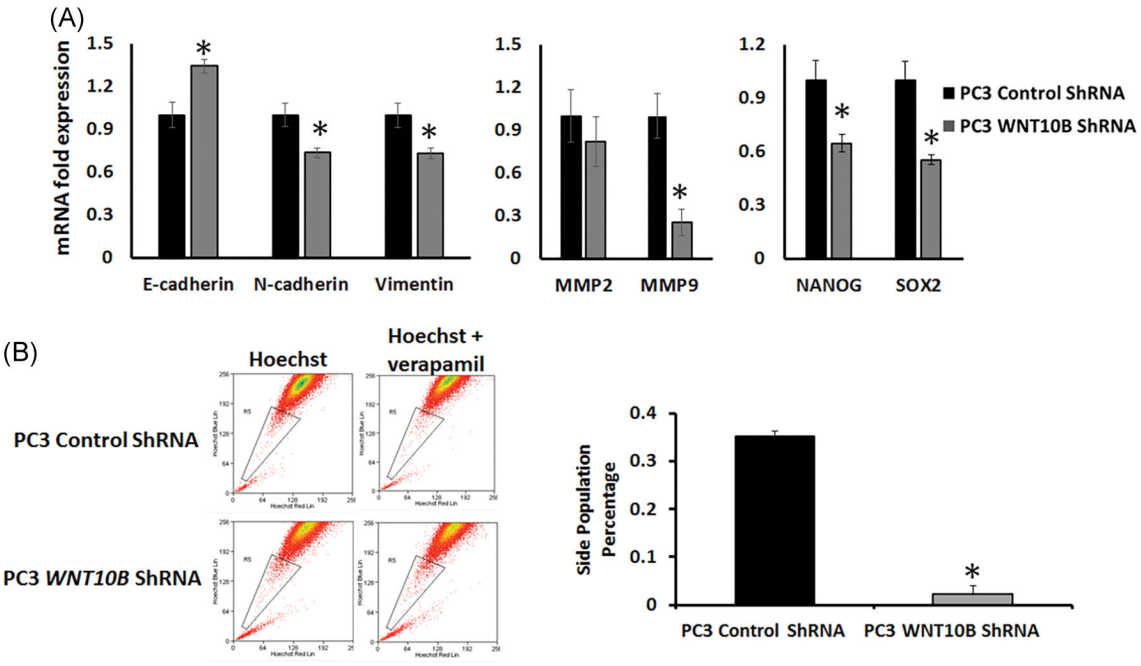

FIGURE 6.

Effect of *WNT10B* knockdown on EMT, metalloproteases and stemness gene expression and the stem-like cell population in PC3 cells. A, PC3 *WNT10B* shRNA cells showed an increased expression of E-cadherin and reduced expression of N-cadherin, vimentin, MMP9, NANOG, and SOX2 compared with control shRNA-PC3 cells. **P* < .05 vs control cells, *N* = 3. Bars represent the mean ± SEM. B, Flow cytometry utilizing a Hoechst exclusion assay was used to assess effect of *WNT10B* knockdown in PC3 cells on the stem-like cell side population. Control shRNA and *WNT10B* shRNA-PC3 cells were stained with 5 μg/mL of Hoechst33342 either in the absence (left) or presence (right) of verapamil hydrochloride 15 minutes before fluorescence-activated cell sorting. The graph represents the percentage side-population cells (gated population) in control shRNA and *WNT10B* shRNA-PC3 cells. Knockdown of *WNT10B* significantly abrogated the stem-like cell side population. **P* < .001 vs control cells, *N* = 4. Bars represent the mean ± SEM. EMT, epithelial to mesenchymal transition; shRNA, short hairpin

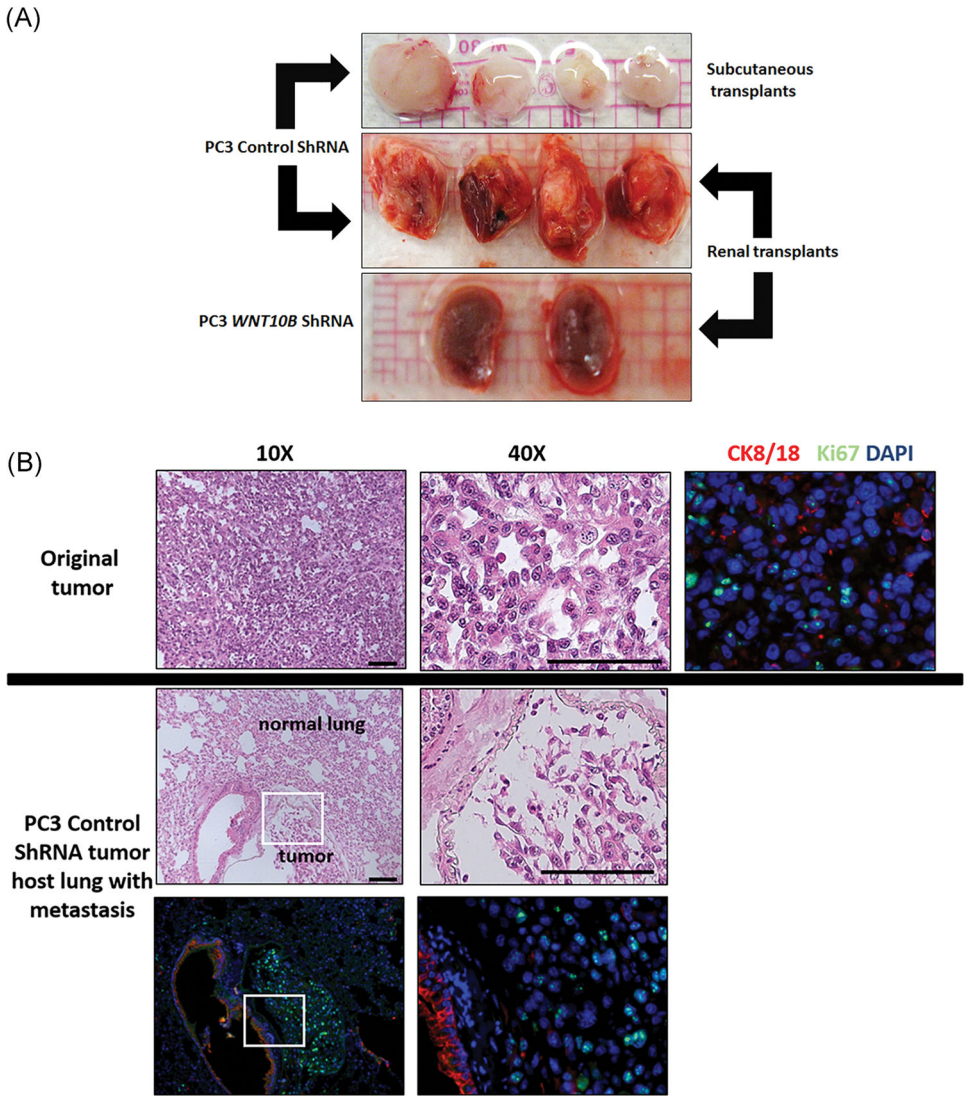

FIGURE 7.

A, Serial transplant of primary PC3 tumor with or without *WNT10B* knockdown. Primary tumors were allowed to form for 30 days using control shRNA or *WNT10B* shRNA-PC3 cells. Tumors were serially transplanted into nude mice hosts either s.c. or beneath the renal capsule and harvested after 9 weeks from s.c. sites (top) or renal site with kidney en masse (middle and bottom). Control shRNA-PC3 primary tumors formed new tumors at both sites (top and middle) whereas *WNT10B* shRNA-PC3 primary tumors were not transplantable at either site. The bottom panel shows kidneys grafted with *WNT10B* shRNA-PC3 primary tumors and only residual 1 mm grafts are visible. Images are representative of $N = 8$. B, Analysis of distant metastasis of PC3 cells in host mice. The top panel shows the primary s.c. tumor generated from control shRNA-PC3 cells with HE staining and immunohistochemistry for CK8/18 (red) and Ki67 (green) revealing poorly differentiated adenocarcinoma. The middle and bottom row images show lung tissue from host mice harboring control shRNA-PC3 metastasis. HE stain (middle) shows normal lung parenchyma with an infiltrated metastatic tumor at ×10 and ×40 magnification. CK8/18

(red) and Ki67 (green) immunostaining (bottom row) shows strong CK8/18 staining in lung epithelium with weaker CK8/18 and Ki67+ cells in the PC3 tumor metastasis. Bottom left is at ×10 and right is at ×40 of the tumor. DAPI, 4′,6-diamidino-2-phenylindole; HE, hematoxylin and eosin; s.c., subcutaneously; shRNA, short hairpin RNA

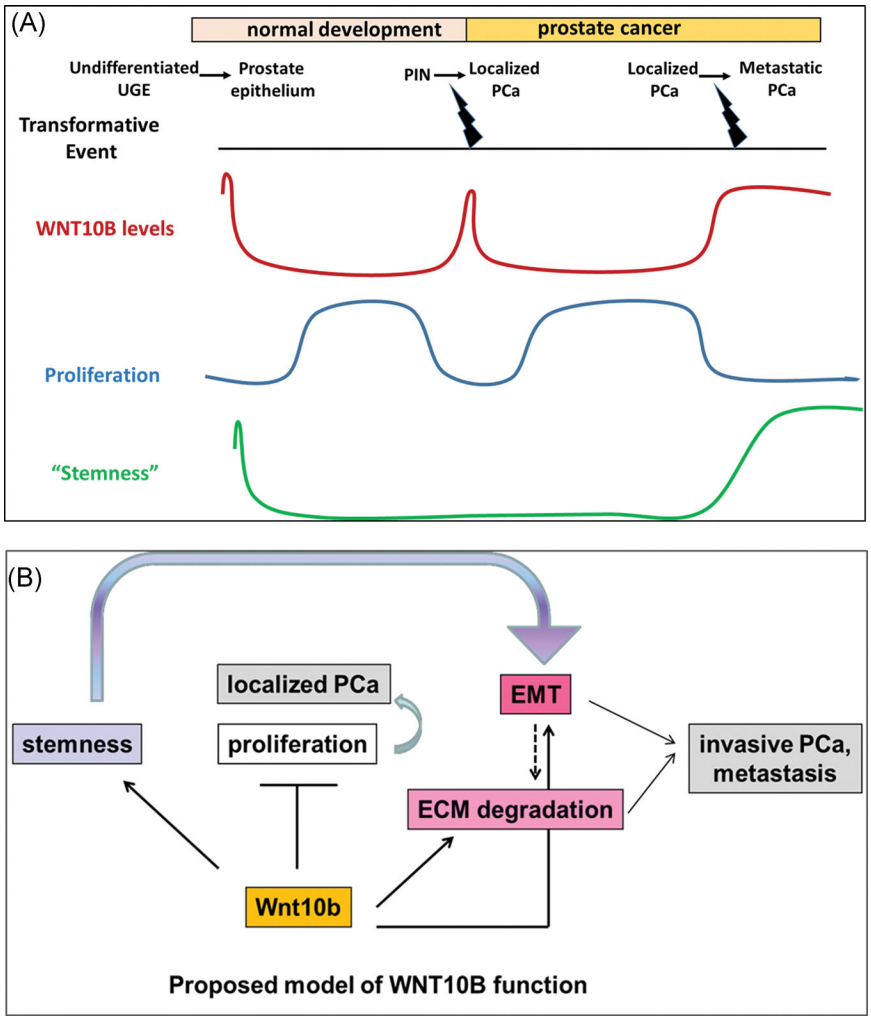

FIGURE 8.

A,B, Proposed model of *WNT10B* action in prostate epithelial cells. Early expression of *WNT10B* is implicated in determination of undifferentiated UGE and rapid decrease to basal levels is necessary to permit controlled and normal prostate gland growth. In localized PCa, a decrease in *WNT10B* levels from PIN to PCa results in loss of *WNT10B*'s antiproliferative function resulting in a hyperproliferative state conducive for tumor formation. As disease advances with dedifferentiation, a stage reminiscent of stem-like undifferentiated epithelium, *WNT10B* is also reexpressed. In this context of advanced disease, loss of *WNT10B* results in a reduction of stemness potential, a reversal of EMT, and ultimately an inability to metastatically propagate tumor growth. ECM, extracellular matrix; EMT, epithelial to mesenchymal transition; PCa, prostate cancer; PIN, prostate intraepithelial neoplasia; UGE, urogenital sinus epithelium